Studies on Aluminum-Isopropoxide Doped Poly(ethylene oxide), Poly(vinyl alcohol), and Poly(ethylene oxide)-Poly(vinyl alcohol) Blends

RACHNA MISHRA, K. J. RAO

Materials Research Center, Indian Institute of Science, Bangalore 560012, India

Received 30 September 1997; accepted 13 January 1998

ABSTRACT: Poly(ethylene oxide), poly(vinyl alcohol), and their blend in a 40 : 60 mole ratio were doped with aluminum isopropoxide. Their structural, thermal, and electrical properties were studied. Aluminum isopropoxide acts as a Lewis acid and thus significantly influences the electrical properties of the polymers and the blend. It also acts as a scavanger for the trace quantities of water present in them, thereby reducing the magnitude of proton transport. It also affects the structure of polymers that manifests in the thermal transformation and decomposition characteristics. © 1998 John Wiley & Sons, Inc. J Appl Polym Sci 69: 2147–2157, 1998

Key words: doping of polymers; poly(ethylene oxide); poly(vinyl alcohol); proton transport

INTRODUCTION

Poly(ethylene oxide) (PEO) and poly(vinyl alcohol) (PVA) form incompatible blends.[1] In the blends PEO influences the ordering of PVA molecules and, this influence manifests in its thermal properties and is evidenced in its vibrational and NMR spectra. However, the electrical properties seem to be far more affected by the presence of trace quantities of water that acts as a source of carriers for the protonic conduction of the blends. The trace quantities of water in the blends originate from the method of preparation. The addition of small quantities of organometallics like aluminum isopropoxide ($Al(^iPr)_3$) can be expected to influence the electrical properties because it can scavenge the trace water and suppress the carrier concentration. Also, the electron deficient aluminum in $Al(^iPr)_3$, which has an inherent tendency to be tetrahedrally coordinated, may act as a Lewis acid and block the etheric oxygen site in PEO. Or it may similarly coordinate to the hydroxyl oxygen on PVA and render the proton in the PVA hydroxyl group available as a carrier.

In this article we report our studies on $Al(^iPr)_3$ doped PEO, PVA, and a PEO : PVA : 40 : 60 blend. Results of the thermal decomposition behavior of the films containing $Al(^iPr)_3$, which lead to formation of oxide residues, are also reported.

EXPERIMENTAL

PEO and PVA were acquired from Aldrich and S. D. Fine Chemicals, respectively. PVA reportedly contained 18% unhydrolyzed acetate. This value was confirmed by the independent chemical analysis carried out using NMR analysis[2] of the methyl and methylene protons and ^{13}C-NMR[3] of the exchanged acetate groups. The molecular weight of PEO was provided by Aldrich ($= 6 \times 10^5$) and that of PVA was determined by the

Correspondence to: K. J. Rao.

Journal of Applied Polymer Science, Vol. 69, 2147–2157 (1998)
 CCC 0021-8995/98/112147-11

Table I Sample Compositions

Sample Code	Compositions (mol %)[a]	
	$Al(^iPr)_3$ with Respect to Monomer	Polymer Reckoned as Monomer
PEO : PVA : 40 : 60		
P1	0.50	0.10
P2	0.70	0.02
P3	1.4	0.01
PEO		
P4	0.07	0.03
P5	0.10	0.07
P6	0.13	0.05
PVA		
P7	0.24	0.10

[a] Percentages were calculated as $x/(x + n_1y_1 + n_2y_2)$ and $ny/(x + n_1y_1 + n_2y_2)$ where x, y_1, and y_2 are the number of moles of the $Al(^iPr)_3$, PEO, and PVA, respectively, and n_1 and n_2 are the number of moles of PEO and PVA.

viscosity method (137,770). The intrinsic viscosity of the PVA solution in water (deionized and double distilled) was determined experimently by measurements of flow times in a standard capillary viscometer. The specific viscosity was used to make a Huggin's plot and η_{sp}/C was extrapolated to zero concentration; C indicates polymer concentration. The intrinsic viscosity η_{intr} was then calculated by using the Mark–Houwink equation, $\eta_{intr} = KM_v^{\alpha}$ where K and α are empirical constants

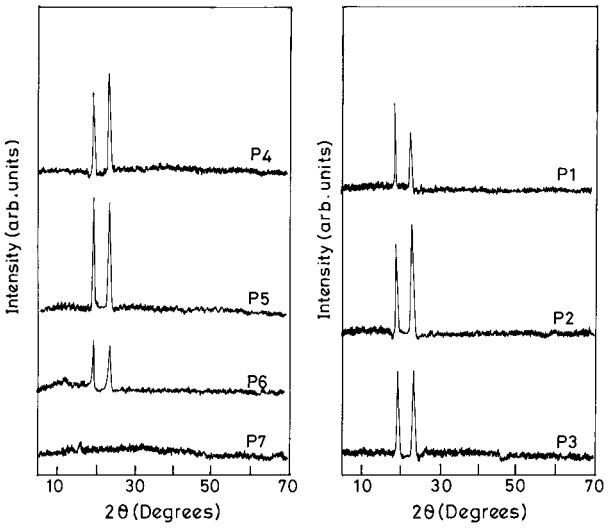

Figure 1 X-ray diffraction pattern of various samples. A describtion of the sample codes are given in Table I.

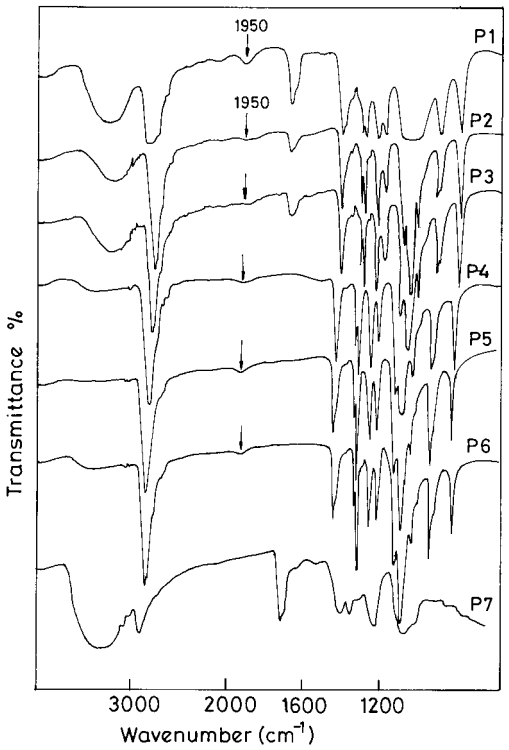

Figure 2 Infrared spectra of various samples.

for the particular system.[4] PEO-$Al(^iPr)_3$ films were prepared by evaporating a mixture of solutions of PEO and $Al(^iPr)_3$, PEO in acetonitrile (dry CH_3CN), and $Al(^iPr)_3$ in dry benzene (C_6H_6). The mixture was stirred for 1 h before evaporation. The cast films were translucent in appearance. Because PVA is insoluble in acetonitrile, films of PEO-PVA blends containing $Al(^iPr)_3$ were prepared first by preparing a solution of PEO and PVA in a 1 : 1 mixture of water : *n*-propanol and adding a benzene solution of $Al(^iPr)_3$ to it. The mixture of solutions had a milky appearence and was continously stirred for 2 h. Films were all cast on Teflon sheets and dried in a vacuum oven at 323 K. The same procedure was adopted to obtain the PVA-$Al(^iPr)_3$ films except that only PVA was present in the water-*n*-propanol solution.

The films were examined using X-ray diffraction (XRD) (Scintag Inc. XDS 2000 XRD machine) using Cu $K\alpha_1$ radiation of wavelength 1.54060 Å and IR spectra (Perkin–Elmer 580 double beam IR spectrometer). Small pieces of the films were cut and loaded into a thermal analyzer to obtain thermogravimetric and differential thermal analyses (Thermal analyzer model STA 1500, Polymer Lab.). A 5°C/min heating rate was employed.

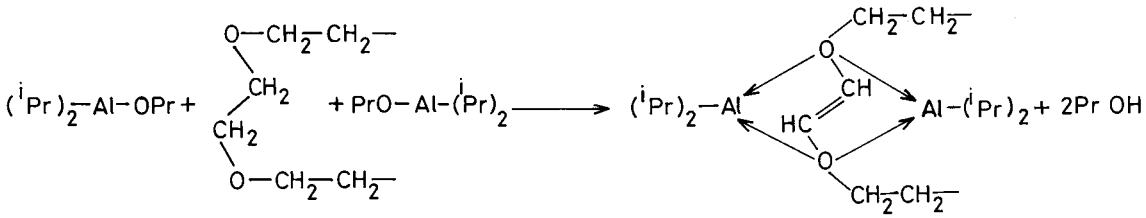

Figure 3 Aluminum isopropoxide-PEO complex formation.

The films generally possessed a highly uniform thickness of around 0.2 mm. Electrodes were sputtered from a gold[5] target over areas of 1 cm^2 and sandwiched between electrodes under gentle pressure using spring loading. The setup along with the connecting lead wires were lowered into the conductivity cell setup whose temperature was controlled accurately to less than 1 K. Temperatures were measured using a thermocouple located close to the sample.

Conductivities were measured using an HP 4192A impedance analyzer. The cell was initially flushed with dry nitrogen to avoid any contamination due to the ambient air. Conductivities were measured from laboratory temperature ($\approx$ 298 K) to 353 K and wherever possible up to 393 K and between 5 and 13.5 $\times$ 10^6 Hz frequency. Conductivities and dielectric quantities could be reproducibly determined only up to about 333 K because PEO melts at this temperature and PVA undergoes a glass transition around the same temperature.

Analysis of Data

The measured capacitance (C_p) and conductance (G) values were used to obtain the real (Z') and imaginary (Z'') parts of the complex impedance. The real and imaginary parts of the complex impedance Z^* ($=Z' + iZ''$) were determined using the relations

$$Z' = \frac{G}{G^2 + \omega^2 C^2} \quad (1)$$

$$Z'' = \frac{C\omega}{G^2 + \omega^2 C^2} \quad (2)$$

The various dielectric data were analyzed using the complex dielectric constant ε^*, complex electric modulus M^*, and complex impedance Z^* of the samples. The conductivity σ and real (ε') and imaginary (ε'') parts of the dielectric constants of the samples were determined using the standard relations;

$$\sigma = Gd/A \quad (3)$$

$$\varepsilon = Cd/\varepsilon_o A \quad (4)$$

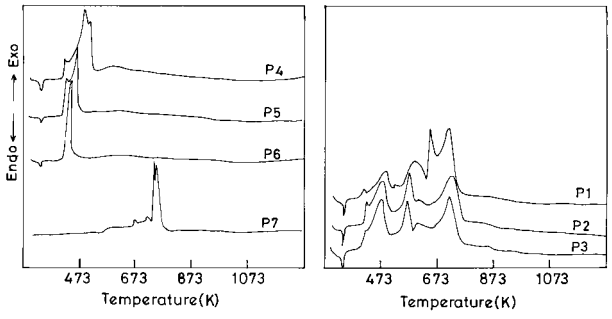

Figure 4 Differential thermograms for different samples.

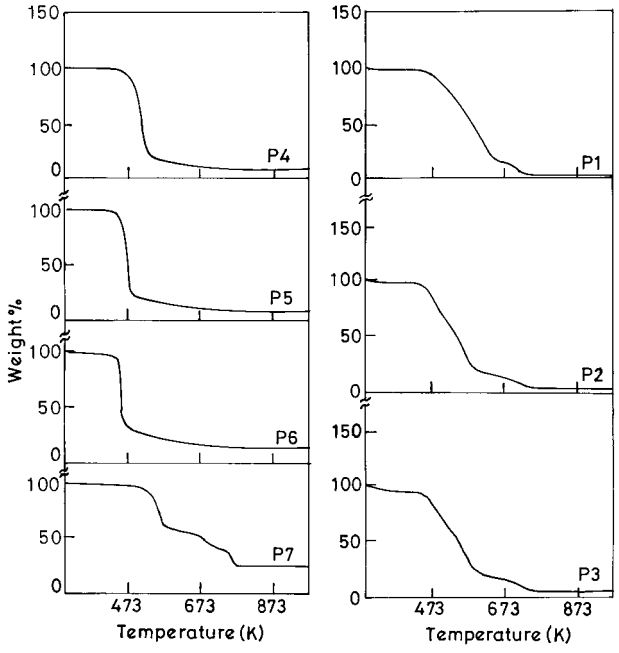

Figure 5 Thermogravimetric curves of various samples.

Table II Initial Decomposition Temperatures Occurring at Various Steps

Sample Code	Decomposition Temperatures (K)				Al_2O_3 Residue (wt %)
	T_1	T_2	T_3	T_4	
PEO : PVA : 40 : 60 + Al(^{i}Pr)$_3$					
P1	473.0	652.0	737.0	—	2.5
P2	463.0	588.0	677.0	—	3.0
P3	460.0	591.0	681.0	—	4.0
Undoped blend	524.0	639.0	—	—	—
PEO + Al(^{i}Pr)$_3$					
P4	471.0	—	—	—	7.0
P5	430.0	—	—	—	11.0
P6	426.0	—	—	—	15.0
Undoped PEO	642.7	—	—	—	—
PVA + Al(^{i}Pr)$_3$					
P7	481.0	566.0	663.0	745.0	25.0
Undoped PVA	529.0	596.0	—	—	—

$$\varepsilon'' = \sigma / w \varepsilon_o \quad (5)$$

where A is the electrode area; d is the thickness of the sample; ε_o is the permittivity of the free space, which is equal to 8.856×10^{-14} F/cm; C is the parallel capacitance; G is the conductance in siemens/centimeter (S/cm); and $\omega = 2\pi f$, f being the frequency in hertz (Hz).

The AC response of the various samples were also studied by the real part of the dielectric modulus (M') and the imaginary part of the dielectric modulus (M''). The complex electric modulus is

$$M^* = 1/\varepsilon^* \quad (6)$$

where

$$\varepsilon^* = \varepsilon' + i\varepsilon'' \quad (7)$$

The real part of the dielectric modulus is given by

$$M' = \varepsilon'/(\varepsilon'^2 + \varepsilon''^2) \quad (8)$$

The imaginary part of the dielectric modulus is given by

$$M'' = \varepsilon''/(\varepsilon'^2 + \varepsilon''^2) \quad (9)$$

RESULTS AND DISCUSSION

The compositions of the films are given in Table I. The molar percentage of Al(^{i}Pr)$_3$ was calculated on the basis of the effective molar concentration of monomers. The molecular weights of the two polymers (PEO = 600,000 and PVA = 137,770) were used for this purpose. To examine the interaction of polymer with Al(^{i}Pr)$_3$, it would be more revealing to consider the concentration of the latter compared to the effective concentration of monomers rather than polymers. This is because every monomer unit has one oxygen atom and the oxygen is the likely center for interaction with Al(^{i}Pr)$_3$.

Structural Studies

XRD patterns of the films are shown in Figure 1. The presence of two reasonably sharp reflections around 19.1° and 23.3° is found to be identical to those observed in undoped films.[1] PVA films did not reveal any diffraction peak in conformity with its amorphous structure. The IR spectra shown in Figure 2 also appear to be largely the sum of the contributions of the spectra of PEO and PVA. Al(^{i}Pr)$_3$ did not give rise to any specific feature in the spectra such as an absorption at 1370 cm^{-1}. This feature is likely to be masked by the dominance of the spectral features of PEO and PVA.[6] The only other significant feature in Figure 2 is that in the spectra of doped PEO films, O—H vibration was not significant and only a shallow depression is observed at $\approx$ 3500 cm^{-1}. Any OH related absorption can be suspected to arise from isopropanol (i-propanol) formed either from the reaction of Al(^{i}Pr)$_3$ with CH_2—O—CH_2 segments or with trace quantities of water. In the former case the abstraction of a proton from CH_2 groups leads to formation

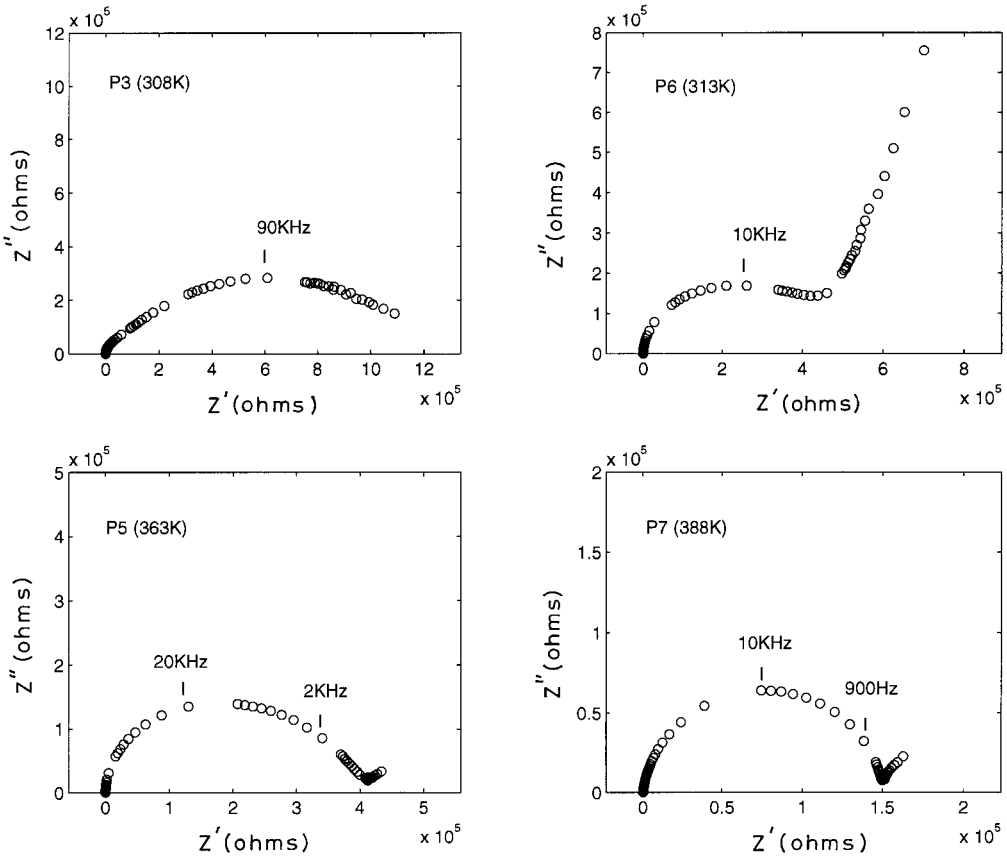

Figure 6 Typical complex impedance plots of various samples.

of *i*-propanol and at the same time provides additional coordination to the aluminum. It is similar to the case of zirconium isopropoxide [7] doping. We presume that the Al(^{i}Pr)$_3$ molecule reacts in the manner shown in Figure 3. Further, the concentration of Al(^{i}Pr)$_3$ is very low, and the probability of accumulation of Al(OH)$_3$ or complexed product molecules of the type shown in Figure 3 is very low. We did not make any further studies to confirm that no clusters containing aluminum were formed. The aluminum atom coordinates itself to oxygen in the PEO chain. It is also possible that the method of preparation unavoidably allows absorption of moisture from the atmosphere that can lead to a slow reaction resulting in the formation of *i*-propanol. A new, but very weak absorption at ν = 1950 cm^{-1} is seen in Al(^{i}Pr)$_3$ doped PEO samples and the blends. The origin of this weak feature is unclear. It cannot be definitely associated with CH bending of the alkenelike structure, particularly in view of the fact that a 1600 cm^{-1} peak is normally associated with alkenes. The absorption peak at 1740 cm^{-1} is present in pure PVA and PVA-rich blends and is due to C=O stretching in unhydrolyzed acetate groups present in the PVA.

Table III dc Activation Energies and Conductivities (at 323 K) of Doped PEO, PVA, and PEO-PVA Films

Compositions (mol %)	E_{a_1} (< 333 K) (eV)	E_{a_2} (> 333 K) (eV)	log σ Extrapolated to ω = 0 (S/cm)
P1	0.22	0.18	−7.90
P2	0.31	0.10	−8.78
P3	0.35	0.13	−8.91
Undoped blend	0.23	0.19	−7.22
P4	0.20	0.07	−7.86
P5	0.16	0.05	−8.70
P6	0.11	0.07	−8.62
Undoped PEO	0.32	0.17	−8.29
P7	0.45	0.13	—
Undoped PVA	—	—	—

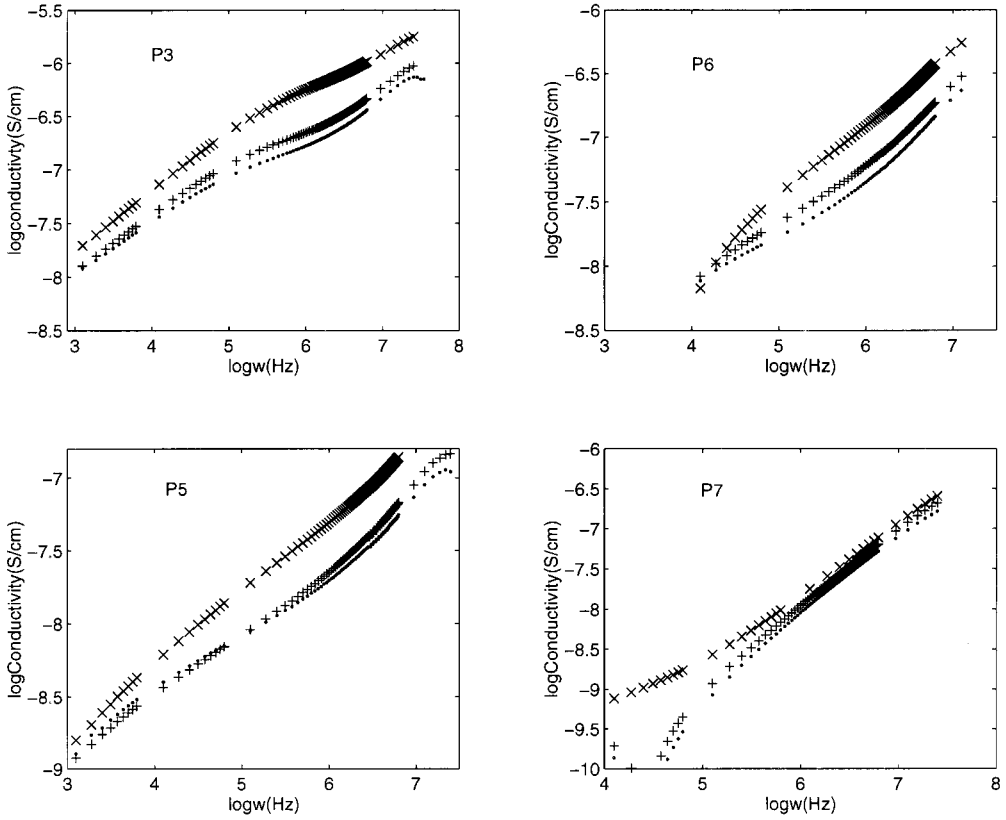

Figure 7 Variation of conductivities (using the power law expression) as a function of frequency (ω) for different samples at ($\cdot$) 303, (+) 313, and 323 ($\times$) K.

Thermal Studies

Differential thermograms of the films are shown in Figure 4. DTA was run using air as the purging gas. The thermograms reveal a number of features; the first endotherm around 333 K can be associated with melting of the PEO in all PEO containing films. It is absent in the DTA of (doped PVA) P7 in which PEO was not present. Pure undoped PVA film prepared from evaporation of a solution of PVA in a 1 : 1 mixture of water and *i*-propanol was found earlier to exhibit an endotherm due to an irreversible order–disorder type transition, and this endotherm was not seen in the DTA of doped PVA samples. Evidently the presence of $Al(^iPr)_3$ molecules that are distributed in the matrix of PVA prevents any ordering of PVA molecules during the film formation. The results of a thermogravimetric analysis (TGA) performed in air are shown in Figure 5. The decompositions appear to be single step and fairly sharp events when either PEO or PVA alone is present. The decomposition events appear to be rather complex in the presence of both PEO and PVA as in the blends P1, P2, and P3. No attempt was made here to analyze the kinetics associated with decomposition. In PEO-$Al(^iPr)_3$ films the major weight loss occurs in sharp steps in the region < 473 K. However, the decomposition continues to occur but slowly above 473 and up to 673 K. Because $Al(^iPr)_3$ also decomposes, perhaps endothermically, leading to gaseous products like propylene in the same temperature region, it was not possible to evaluate any thermodynamic quantities. In Table II temperatures corresponding to the beginning of various decomposition steps are given and compared with those observed in undoped PEO, PEO-PVA blends, and PVA. The weight percents of the alumina (Al_2O_3) residue obtained at 1273 K are also listed. It is evident from Table II that the decomposition characteristics are substantially affected by the presence of $Al(^iPr)_3$ in all cases. This could be a consequence of the manner in which the polymer locked $Al(^iPr)_3$ molecules are dispersed in PEO, PVA, and PEO-PVA matrices. The mode of decomposition can be expected to be affected because of the localized absorption or release of heat by the or-

Table IV Double Power Law Values of A_1, A_2, s_1, and s_2 at Temperatures < 338 K

Sample Code	Temperature (K)	s_1	log A_1 (S/cm)	s_2	log A_2 (S/cm)	log σ_{ac} (1 MHz) at 323 K (S/cm)
P1	303	0.55	−10.29	0.21	−9.96	—
	313	0.57	−10.67	0.29	−10.03	—
	323	0.56	−10.67	0.29	−10.13	−7.93
P3	303	0.46	−9.39	0.39	−9.05	—
	313	0.47	−9.73	0.37	−9.05	—
	323	0.49	−10.30	0.32	−8.79	−6.44
Undoped PEO : PVA : 40 : 60	313	0.49	−9.49	0.34	−9.30	−6.05
P5	303	0.56	−10.64	0.25	−10.04	—
	313	0.51	−10.65	0.25	−10.15	—
	323	0.50	−10.66	0.29	−10.15	−7.26
P6	303	0.47	−12.02	0.56	−10.24	—
	313	0.49	−10.18	0.45	−10.74	—
	323	0.50	−10.22	0.39	−11.05	−6.76
Undoped PEO	313	0.41	−9.51	0.31	−9.69	−6.66
P7	303	0.99	−13.00	0.1	−12.00	—
	313	0.88	−12.15	0.19	−10.00	—
	323	0.88	−12.15	0.20	−10.00	−7.07
Undoped PVA	313	0.93	−12.66	0.30	−10.70	−6.47

ganic moieties. Al(^{i}Pr)$_3$ molecules may be acting as heterogenous nucleation centers for the decomposition of the polymers; as a consequence, the decomposition temperatures are much lower in all systems. Al(^{i}Pr)$_3$ molecules locate themselves in the polymer matrix in such a way that aluminum atoms acquire the preferred four coordination to oxygen. Therefore, either C—O—C segments of PEO or OH groups of PVA come close to the Al atom in the structure. We should also expect the resulting molecular configurations to influence both the concentrations and the mobilities of protons available for conduction and the dielectric relaxation characteristics of the polymers. These aspects are discussed later.

dc Conductivity

The dc conductivities were determined using impedance plots. A few typical impedance plots are shown in Figure 6. Impedance plots with reproducible values Z' (the real part) and Z'' (the imaginary part) of the impedances covering at least half of the semicircle in Cole plots could be obtained only above 323 K. This was surprising because in the undoped PEO, PVA, and PEO-PVA blends the reproducible impedance plots could be obtained only below 333 K. In this investigation we were interested in only the behavior of the two polymers and their blends below 333 K. We calculated a few activation barriers from the analysis of the data above 323 K also, and they (designated as E_{α_2}) are given in Table III. The activation barriers are rather low above 323 K.

Because the impedance plots were unsatisfactory below 323 K, the dc conductivities were determined from the extrapolation of ac conductivities to $\omega = 0$, but for measurements done over a limited temperature range below 333 K (typically 308–328 K). Such extrapolation procedures generally lead to less satisfactory results than those obtained from impedance plots. These conductivity measurements were used to determine the activation barriers in doped and undoped compositions, and they are also listed as E_{α_1} in Table III for comparison. The dc activation barriers below 333 K were lower in doped PEO films compared to the undoped PEO film. We assumed in this work that the charge carriers are only protons. The carriers cannot be electrons because it implies excitation of electrons across a band gap. The band originates from the highest occupied molecular orbitals of oxygen atoms (lone pair levels of oxygen) and the lowest unoccupied molecular orbitals (corresponding to the antibonding levels of C—O bonds). These gaps are expected to be much higher (several electron volts); therefore, we feel that the charge carriers are only protons. Protons probably originate from very low impu-

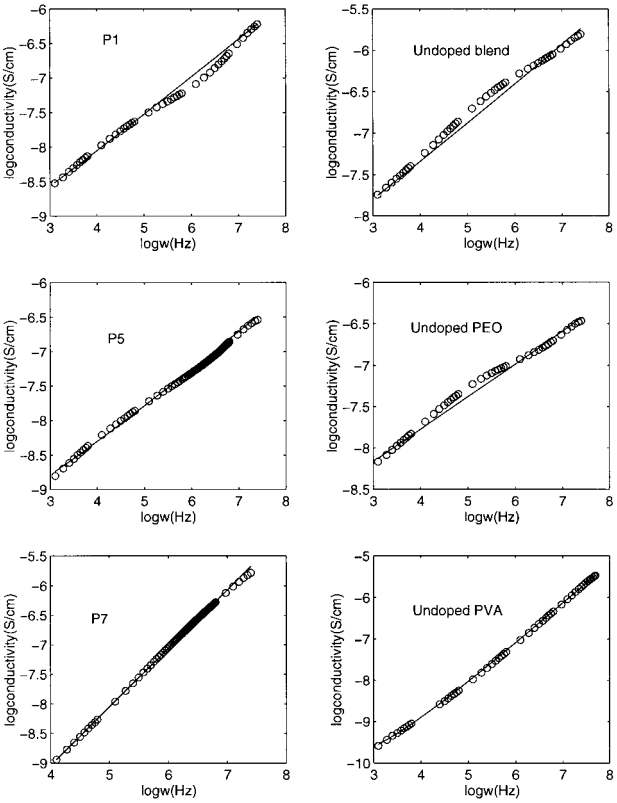

Figure 8 Typical power law fits [(○) experimental and (—) fit to the data] for different samples at (○) 303 K.

rity level water molecules or from the OH groups that result from the ether-enol equilibration of the end of the etheric chain linkages in pure PEO. The concentration of charge carrier is as low as 10^{14}/mL when the mobilities are assumed to be typical at about 10^{-4} cm^2/V s, which is a very small concentration. The observed behavior of the activation barrier is also consistent with the possible role of oxygen (both the etheric oxygen in PEO and the hydroxy oxygen in PVA) in proton transport. In undoped compositions protons hop from oxygen to oxygen, which act as a hopping center. But when $Al(^iPr)_3$ is present in the composites, these oxygen atoms are coordinated to Al atoms; therefore, protons disengage from them and to that extent lower the effective barrier to transport (see later discussion). But the dc conductivities themselves are lower (see Table III) in doped films than in undoped films. We attribute this to the H_2O scavenging effect of $Al(^iPr)_3$. H_2O reacts with the isopropoxide, which is a (delayed) hydrolysis, thereby decreasing the number of protons available for transport.

ac Conductivity

Variation of $\sigma(\omega)$ with ω is shown in Figure 7 in log–log plots. However, these conductivities have been corrected using the (not so accurate) dc conductivities obtained from the impedance plots. The corrections are therefore unlikely to be accurate for the reasons mentioned above. In the range of frequencies covered in the present measurements, the data were analyzed with a power law expression[8–10] of the form

$$\sigma(\omega) = A_1\omega^{s_1} + A_2\omega^{s_2} \qquad (10)$$

The fitting procedures ensure that wherever the single power law was sufficient, s_1 is set equal to s_2 or A_2 to zero. The fitting parameters are summarized in Table IV for typical doped polymers. Similar parameters obtained at 313 K for undoped polymer compositions are also given in the Table IV. A few typical plots showing the fitting of the data are presented in Figure 8. It may be noted that over short regimes of frequency the fitting to eq. (10) is poor in some cases. The following observations can be made. The bilinear variation

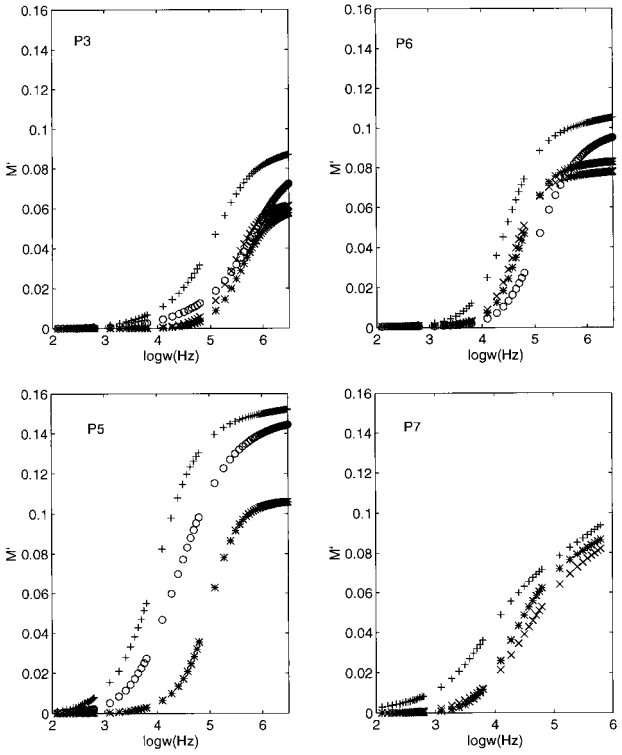

Figure 9 Typical plots of the variation of the real (M) part of the dielectric moduli (M^*) with frequency at various temperatures: (○) 303, (+) 323, (×) 353, and (★) 373 K.

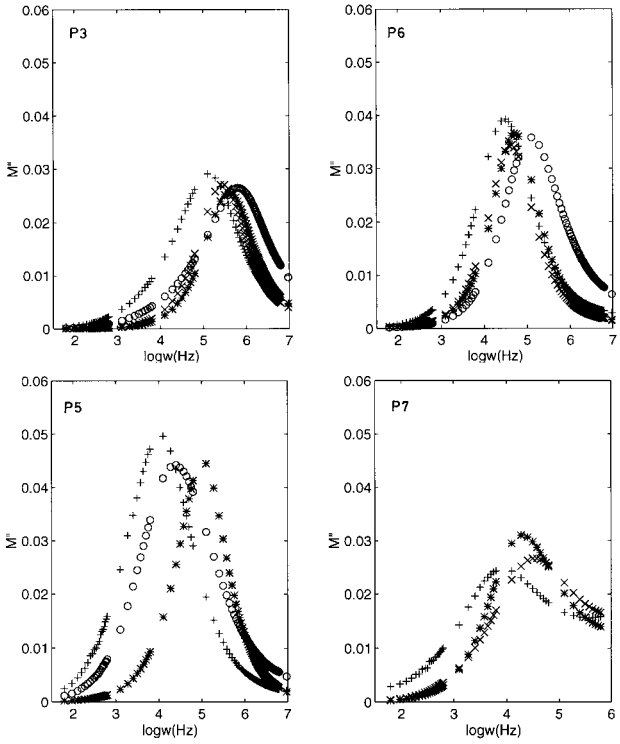

Figure 10 Typical plots of the variation of the imaginary (M'') part of the dielectric moduli (M^*) with frequency at various temperatures: (○) 303, (+) 323, (×) 353, and (★) 373 K.

of the ac conductivity is common to both pure PEO and doped PEO films. However, the magnitudes of s_1 and s_2 of doped films are significantly higher than in pure PEO films. A_1 and A_2 are also significantly lower (log A_1 and log A_2 being more negative) than in undoped films, indicating a lower value of ac conductivity.

Although just a single term power law expression (A_1 and s_1) could be used in the doped PVA films, it was found that the two term power law provided better fits, and the parameters are given in Table IV. Values of s_1 were rather high (closer to unity) in doped and pure PVA samples. Doping also affects σ_{ac} values to a lesser extent, and it is lower in the doped samples. The s_1 and s_2 values are closer to those of PEO at the low concentration of the dopant but increase to values similar to s_1 and s_2 values of PVA at the higher concentration of the dopant. But the data at present is insufficient to draw further inferences. However, in general the conductivities are also lower in the presence of dopant in the blends. The span and the trends of s_1 and s_2 therefore suggest that the mechanism of proton transport remains essentially unaffected, but the carrier concentration or number of protons available for transport is somewhat reduced. This appears to be a manifestation of the water scavenging effect of Al(^{i}Pr)$_3$. The isopropoxide reacts with traces of water present in the film.

Dielectric Behavior

To further investigate the effect of doping on ac phenomena, we analyzed the dielectric behavior using a modulus representation. The variation of M' and M'' of the films discussed above are shown in Figures 9 and 10, respectively. At low frequencies a rather intense rise in the real part of the dielectric constant was observed, which is reflected in the low frequency regime of M'. This is due to electrode polarization and/or space charge effects that are known to occur in polymer films. Even in the small range of temperature over which dielectric properties were measured for these films we noted a variation in the heights of the M'' peaks. As shown in Figure 11, the superposition of reduced plots was not satisfactory in either single component or blend films doped with Al(^{i}Pr)$_3$. This is contrary to the behavior in undoped films in which the superposition was quite

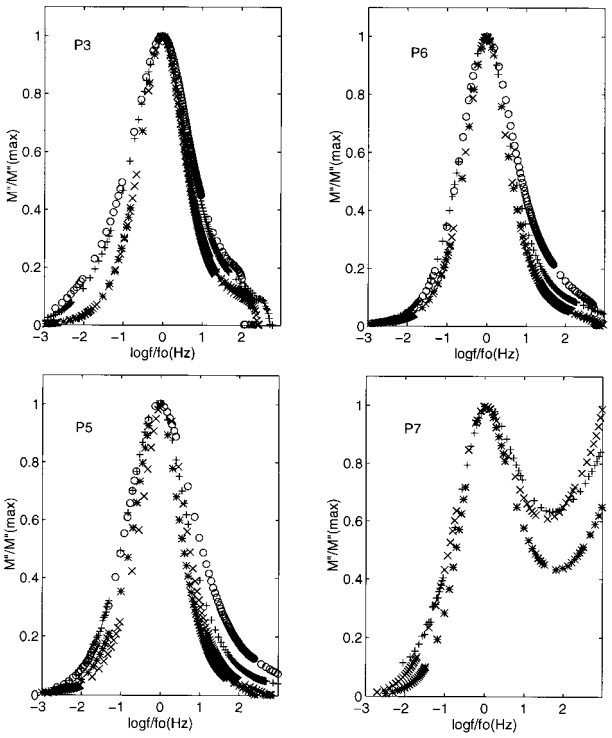

Figure 11 Typical plots of normalized M'' against normalized frequency at different temperatures: (○) 303, (+) 323, (×) 353, and (★) 373 K.

Table V FWHM and β Values for Several Doped Films

Samples (mol %)	Temperature (K)	FWHM Decades of Frequency	β	τ (s)
P3	303	1.91	0.57	1.00×10^{-5}
	313	1.83	0.60	3.38×10^{-5}
	323	1.80	0.61	5.01×10^{-5}
Undoped PEO : PVA : 40 : 60	313	2.00	0.54	1.00×10^{-5}
P5	303	2.06	0.53	2.53×10^{-4}
	313	1.93	0.57	6.36×10^{-4}
	323	1.83	0.64	5.01×10^{-4}
P6	303	1.68	0.66	5.01×10^{-5}
	313	1.62	0.68	1.43×10^{-5}
	323	1.56	0.71	2.06×10^{-4}
Undoped PEO	313	1.87	0.59	2.47×10^{-5}
P7	313	2.53	0.43	2.89×10^{-3}
	323	2.24	0.49	7.05×10^{-4}
Undoped PVA	313	2.29	0.47	1.90×10^{-2}

FWHM, full width at half maximum.

satisfactory. The relaxation peaks in M'' were examined using a stretched exponential relaxation function[11] of the type

$$\Phi(t) = \Phi_o \exp(-t/\tau)^{\beta} \qquad (11)$$

where Φ is any property (e.g., a dielectric function) and β is the parameter that serves as a measure of the stretching of the relaxation times as the relaxation progresses. Values of β were determined from the standard interpolation method[12,13] and are given in Table V. The full width at half maximum in doped PEO is higher in undoped films when the level of doping is low but lower at higher dopant concentrations. The difference in the β values of doped and undoped films was not very significant in PVA. In the doped films there was also no evidence of two different relaxation peaks in the blends. Although the dopant interacts differently with PEO and PVA, the relaxation spectra do not reflect well-separated relaxation peaks. The relaxation times are much lower (2 orders of magnitude) in doped PVA films ($\tau = 2.89 \times 10^{-3}$ s at 313 K) compared to doped PEO films ($\tau = 1.4 \times 10^{-5}$ s) at 313 K (see Table IV). This is perhaps a reflection of the fact that in PEO the polarization relaxation caused by the jump of protons between etheric oxygen is characterized by a much smaller barrier (lower interaction energy between oxygen and protons), while it is higher between protons and alcoholic oxygen in PVA.

Table I shows that the proportion of the dopant $Al(^iPr)_3$ present in the films is less than 1.0%. If the effect of the dopant arises primarily from the oxygen coordination requirement of Al atoms in $Al(^iPr)_3$, it appears that there should be very little influence of the dopant on the transport and dielectric behavior of the polymer films because monomers of PEO and PVA can provide an oxygen each and therefore large portions of polymers must remain unaffected. It is therefore necessary to consider the possibility of the dopant $Al(^iPr)_3$ molecular being able to disturb a much larger number of sites involved in transport and segments involved in dielectric relaxation. Because the isopropoxide unit $(CH_3—CH(CH_3)—O—)_3—$ is significantly larger than either EO or VA groups of the host polymers and because every dopant molecule comes with three isopropoxide groups, it is likely that an entanglement region of a much larger size than the monomers is created in the doped samples. This is supported by thermal measurements because in doped films the irreversible order–disorder transition endotherm observed in solution prepared PVA is absent, because such regions of molecular entanglement prevent ordering. Further, the decomposition characteristics of the polymer films in general are also profoundly affected in the presence of the dopant.

CONCLUSIONS

Aluminum isopropoxide added as a dopant to PEO, PVA, and PEO-PVA blends causes remark-

able changes in the behavior of the host polymers. Thermal decomposition, electrical conductivity, and dielectric studies reveal that the dopant has a significant interaction with host matrices and acts as a scavenger for the traces of water that are sources of protons for ion transport.

The authors acknowledge the help of Dr. Bhaskaran in fitting the data to standard expressions.

REFERENCES

1. R. Mishra and K. J. Rao, personal communication.
2. G. V. Velden and J. Beulen, *Macromolecules,* **15,** 1071 (1982).
3. T. K. Wu and M. L. Sheer, *Macromolecules,* **10,** 529 (1977).
4. J. Bandrup and E. H. Immergut, *Polymer Handbook,* 2nd ed., Wiley Interscience, New York, 1975, p. 15.
5. G. S. Rellick and J. Runt, *J. Polym. Sci.: Part B: Polym. Phys.,* **26,** 1425 (1988).
6. C. N. R. Rao, *Chemical Applications of Infrared Spectroscopy,* Academic Press, New York, 1963, Chap. 2.
7. P. Jundeinstein and C. Sanchez, *J. Mater. Chem.,* **6,** 511 (1996).
8. D. P. Almond and A. R. West, *Solid State Ionics,* **23,** 27 (1987).
9. M. Siekierski and W. Wieczorek, *Solid State Ionics,* **60,** 67 (1993).
10. S. R. Elliot, *Solid State Ionics,* **70/71,** 27 (1994).
11. R. Kohlrausch, *Ann. Phys. (Leipzig),* **12,** 393 (1847).
12. C. T. Moynihan, L. P. Boesch, and N. L. Laberge, *Phys. Chem. Glasses,* **13,** 171 (1972).
13. C. T. Moynihan, L. P. Boesch, and N. L. Laberge, *Phys. Chem. Glasses,* **14,** 122 (1973).